PROTON RADIOGRAPHY*

G. E. Hogan#, K. J. Adams, K. R. Alrick, J. F. Amann, J. G. Boissevain, M. L. Crow, S. B. Cushing, J. C. Eddleman, C. J. Espinoza, T. T. Fife, R. A. Gallegos, J. Gomez, T. J. Gorman, N. T. Gray, V. H. Holmes, S. A. Jaramillo, N. S. P. King, J. N. Knudson, R. K. London, R. P. Lopez, J. B. McClelland, F. E. Merrill, K. B. Morley, C. L. Morris, C. T. Mottershead, K. L. Mueller, Jr., F. A. Neri, D. M. Numkena, P. D. Pazuchanics, C. Pillai, R. E. Prael, C. M. Riedel, J. S. Sarracino, A. Saunders, H. L. Stacy, B. E. Takala, H. A. Thiessen, H. E. Tucker, P. L. Walstrom, G. J. Yates, H.-J. Ziock, J. D. Zumbro, LANL, Los Alamos, NM 87545

E. Ables, M. B. Aufderheide, P. D. Barnes Jr., R. M. Bionta, D. H. Fujino, E. P. Hartouni, H.-S. Park, R. Soltz, D. M. Wright, LLNL, Livermore, CA 94550

S. Balzer, P. A. Flores, R. T. Thompson, Bechtel, Nevada, Los Alamos Operations, Los Alamos, NM 87545

A. Pendzick, R. Prigl, J. Scaduto, E. T. Schwaner, BNL, Upton, NY 11973

J. M. O'Donnell, University of Minnesota, Minneapolis, MN 55455; current address: LANL

Abstract

With the nuclear weapons program moving to Science Based Stockpile Stewardship (SBSS), new diagnostic techniques are needed to replace weapons testing. Proton Radiography [1] is being developed within the SBSS program as one such tool. It is analogous to transmission X-ray radiography, but uses protons instead of photons. Proton Radiography has high penetrating power, high detection efficiency, small-scattered background, inherent multi-pulse capability, and large standoff distances between test objects and detectors. Multiple images on a single axis through progressively smaller angle-cutting apertures can provide material identification. Proton Radiography can make multi-axis, multi-frame radiographs: i.e., 3D radiographic movies. This approach to SBSS is being developed at the Los Alamos National Laboratory (LANL) and the Lawrence Livermore National Laboratory (LLNL). This new method of radiography, as well as radiography experiments performed at the LANSCE accelerator at LANL and at the Alternating Gradient Synchrotron (AGS) at Brookhaven National Laboratory, will be discussed in this paper.

1 INTRODUCTION

The SBSS program supports a weapons maintenance system based on detailed knowledge of the underlying physics as opposed to the performance based system of underground nuclear tests. An essential class of experiments in understanding the underlying physics of weapons is the hydrodynamic test (or hydrotest). The goal of these experiments is to understand how materials behave at the high temperatures and pressures generated by explosively driven pressure or shock waves. Obtaining high-quality data from such hydrotests is one of the main goals of SBSS.

Previously, weapons physics was addressed through a combination of weapons tests, hydrotests, and computer simulations. However, with the Comprehensive Test Ban Treaty, hydrotests and simulations are now the principle tools available for certifying weapons performance. Current simulations must be upgraded to include 3D effects from a) manufacturing defects, b) ageing, and c) safety tests. Hydrotests are needed to validate the simulations.

Multiple views are needed to handle 3D shapes (tomographic reconstruction) and multiple times (movies) to understand when perturbations become important and how they develop over time. This is the purpose of the proposed Advanced Hydrodynamic Facility (AHF), which is intended to provide hydrodynamic test data of sufficient precision to allow the certification of the weapons stockpile in the absence of underground testing. An AHF based on proton radiography can contribute to a full 3D understanding of the hydrodynamic problem within the SBSS program.

2 PRINCIPLES OF PROTON RADIOGRAPHY

In weapons X-ray radiography, a sharp image is formed because the X-rays start out at a small spot and travel in straight lines through the radiographed object to the X-ray film or detector, basically a variation on the pinhole camera. Images made in the same way with protons as with X-rays, using no lenses, would be blurred by the

0-7803-5573-3/99/$10.00@1999 IEEE.

multiple Coulomb scattering (MCS) of the protons from the charged nuclei of the object. In proton radiography, the effect of this blurring is mostly eliminated by passing the emergent proton beam through a series of magnetic lenses [2] that focus the proton beam to an image of the object at a distance of 20 to 100 meters away from the object itself. This approach is similar in principle to that used in ordinary visible-light cameras.

The three most important effects on the protons as they go through an object are absorption, multiple Coulomb scattering, and energy loss. First, some of the protons are absorbed by nuclear collisions. This is a simple exponential attenuation of the beam. Second, the protons are scattered into small angles by multiple Coulomb scattering. This not only produces image blurring, but it also changes the total attenuation as a detector may not see the full phase space of the scattered beam. Third, protons lose varying amounts of energy as they go through an object from both energy straggling and thickness variations in the object. This produces a spread in the momentum of the transmitted protons that blurs the final image due to chromatic aberrations in the lens.

The proton attenuation length in heavy metals is around a few hundred gm/cm^2, which makes proton radiography well matched to the AHF class of problems, and allows use of the minimum amount of beam (or dose) on the object. This reduces scattered background and multi-axis crosstalk. In addition, the penetrating power of protons and the fact that they are charged particles means that a single proton can pass through multiple thin detectors and be detected in all of them with high probability. This feature can be used to advantage to form multiple images when magnetic identity lenses and detector systems are placed in series downstream of the object.

3 LENS SYSTEM AND MATERIAL IDENTIFICATION

Protons that are not scattered or absorbed in the object emerge from the object with a reduced energy due to collision with atomic electrons and an energy spread due to both energy straggling and thickness variations in the object. This energy spread, together with chromatic aberrations in the lenses, causes image blurring. Chromatic aberrations in the magnetic lenses can be minimized by making the lens system as short as possible and by use of an illuminating beam with a special correlation between transverse position and angle. The lens is an inverting, unit-magnification lens. Thus, the relation between object position and image position is

$$x_{image} = -x_{object} + \text{aberration terms}$$

Including only the two aberration terms in the final position of the proton that depend in first order on the momentum variation, relationship is:

$$x_{image} = -x_{object} + (x \mid \theta\delta)\theta_{obj}\delta + (x \mid x\delta)x_{obj}\delta$$

where δ is the fractional momentum difference from the design momentum of the lens, x the lateral position of the proton at the object, and θ the angle with respect to the central axis of the lens. The items in parenthesis are aberration coefficients given by the lens design codes. Higher order terms are not shown. In the first aberration term, the momentum difference multiplies the angle at which the proton goes through the object. In the second term, the momentum difference multiplies the position of the proton at the object.

One can eliminate the position dependence of the second-order chromatic aberration by imposing the condition:

$$(x \mid \theta\delta)\theta_{object} = -(x \mid x\delta)x_{object}$$

on the incoming proton-beam phase space. With this special correlation, the only second-order chromatic blurring left in the image plane is due to the deviations from this angle due MCS.

This correlation also causes unscattered rays to come to a point focus at the center of the lens. Scattered protons are imaged away from the point with a distance proportional to the MCS angle. A collimator placed here can make cuts on this angle. Another effect of this correlation is to dramatically increase the field of view of the lens system.

Proton radiography offers the unique feature of material identification, in which regions in the test object made up of lighter atoms can be distinguished from regions made up of heavier atoms. Material identification is done by comparing two same-sized images of the same view that are formed at the same time by placing two identity lens and detector systems in series. An angle filter placed in the middle of the second lens system makes cuts on the MCS angle distribution of the protons that emerge from the object. Since nuclear attenuation has an $A^{2/3}$ dependence, whereas the r.m.s. MCS scattering angle varies as Z^2, the heavier atoms in the radiographed object contribute relatively more to the contrasts in the second image than in the first image.

A third lens upstream of the object allows an independent measurement of the intensity distribution of each proton pulse in the illuminating beam. This information can be used to correct for pulse-to-pulse variations in the beam position and shape. It also improves the statistical power of the measurement, as one knows the exact input density of protons at each point in image.

Scattering from the containment vessel that holds the object under test also affects the position resolution at the image plane and is not removed by the lens system. The containment vessel is needed for two reasons: first, to protect the equipment from several pounds of exploding HE; and second, to confine any hazardous material used in the experiment. The effect of this containment wall scattering scales inversely with the momentum of the proton beam and drives the final design energy of an AHF proton accelerator to the range of 50 GeV.

4 DETECTORS

The detection systems used in Proton Radiography are as important as the design of the beam. Ideally, what we want is a method to take good resolution pictures (< 1 mm FWHM) at a high frame rate (≥ 5 MHz). A common feature of these detectors is that they use the energy loss of protons through a detection medium to achieve almost 100% detection efficiency for individual protons. High efficiency minimizes the radiation dosage needed to achieve a given statistical accuracy. Because of the high instantaneous beam intensity (>10^4 protons per mm^2 in a 50 ns pulse), the detectors are all integrating devices rather than counting devices. We are working on a number of detection schemes that address these requirements.

4.1 Image Plates

Image plates are very similar to film. They are sheets of a metastable phosphorescent material that is directly exposed to the proton beam. As a proton passes through the plate, it excites metastable states in the plate material. The amount of material that is excited is proportional to the exposed proton flux. A laser scanner is used to measure this excitation. The chief practical difference with film is that the image plate is reusable. It produces very high-resolution images (~100 micron/pixel). It is also an order of magnitude more sensitive and very linear in its response to protons. Its chief advantage is that it produces very low cost, very high-resolution images. Our better than one line pair per millimeter resolution is limited by the beam optics, not the detector. Unfortunately, there is no practical way to make a movie with image plates. This is the detector of choice for static objects, such as a limited view tomographic reconstruction of a stable object.

4.2 Electronic Camera Systems

The present method for obtaining a sequence of images for dynamic experiments is to use a number of gateable, intensified CCD cameras [3]. One obtains an image by gating the CCD to turn on when the proton beam goes through a scintillating fiber optic array. The CCD camera is fiber-optically coupled to a fast gated (≥50ns) planar diode with a photocathode spectral response matched to the scintillator light output. We have used a variety of CCD arrays ranging in size from 512^2 to 2048^2 pixels. We have also used microchannel-based intensifiers in place of the planar diodes.

We get several pictures at different times by having several cameras pointed at the same scintillator with each camera gate timed to a different proton pulse. In our current tests, the pulses are usually spaced at one-microsecond intervals. The cameras view the scintillator via a series of mirrors. The scintillator is a close packed array of scintillating fibers (300micron core) aligned in the proton beam direction.

We have used up to eleven cameras at once. A prototype four-frame framing camera is currently under development. Available real estate for cameras restricts the number of frames per image plane. Optical coupling efficiency in the present lenses limits the statistics in the images obtained with this technique. Future possibilities include advanced CCD camera designs which permit multiple “on chip” frame storage. These designs would allow for very fast framing speeds and a large number of frames from a single camera. A solid state streak camera that uses 128 photodiodes and takes 512 frames at rates up to six million frames per second is being tested by LLNL.

4.3 Silicon Detectors

Another technology we are developing is direct detection using a solid state device with individual pixel readout. This work is being done with Lawrence Berkeley National Laboratory (LBNL). Conceptually, it is similar to putting a CCD directly in the beam. In this case the detector elements are much thinner and the readout scheme much faster. An 8 × 8 pixel prototype was been tried and has successfully taken a 1000 frame movie. The pixels were 1 mm^2. We hope to test a 100 × 100 pixel system next year. The main problem with this is that there is a systematic noise problem caused by nuclear interactions of the protons with the 3.5 μm thick silicon pixels. Thus the in-beam detector may not be useful, but the readout electronics being developed along with it will be tested in a lens to fiber array to silicon pixel coupling scheme.

4.4 Ion Chambers

A way around the nuclear interaction problem may be to use an ionization chamber with hydrogen gas instead of silicon as the detection media. Nuclear fragmentation is then not a problem. The ionization charge would be collected on a pixelated cathode plane. We will probably use the same high volume analog to digital conversion electronics being developed for the silicon detectors described above.

4.5 Cherenkov Detectors

When a charged particle travels through material, it loses energy in addition to being absorbed. We can detect this energy loss by measuring the Cherenkov radiation from protons. For 800-MeV protons, the index of refraction for the threshold of Cherenkov light production is 1.188. This index is not readily available from common materials. We fabricated the required material using high-density aerogel radiators. Once the light is produced, detection schemes are similar to the CCD camera system. This detector system is particularly useful for imaging very thin objects where the absorption of the beam is small. This is primarily being developed by LLNL [4]. This might allow low dose radiography of living objects.

4.6 Data Acquisition (DAQ) System

All of the various data streams are brought together into one DAQ program. The program is called PC DAQ [5] and it is a Windows® based general DAQ/Analysis/Monte Carlo shell developed as part of the Proton Radiography project. It integrates data from picture files, GPIB devices (scopes, pulsers, etc.), ActiveX servers, and CAMAC modules. In our latest round of measurements, it used or acquired data from 12 PC workstations. This program has been adopted as the principal DAQ system for several experiments outside of the Proton Radiography project. It is currently in use with experiments at Brookhaven National Laboratory (BNL) and LANSCE.

5 EXPERIMENTS

In 1996, we radiographed a test object known as the French Test Object (FTO) [6] with a 10-GeV proton beam at the AGS at BNL using a radiographic single-lens system. The object is made of spherical layers of different materials. It has a hollow cavity in the center, surrounded by layers of tungsten, copper, and finally foam. This experiment demonstrated proton radiography's spatial and density reconstruction capability.

Figure 1 shows two lineouts from image plate radiographs taken with different collimator cuts on the scattering angle. Each image integrated about 10^7 protons over several hours. Using the differences in the two line shapes, we have derived the separate nuclear and electromagnetic interaction lengths that go into the absorption equation. The derived values (Table 1) agree well with the published values.

Table 1, Fitted Results to the FTO Measurement

	Radius (cm)		Nuclear Attenuation (cm)		Radiation Length (cm)	
Shell	Actual	Fit	Actual	Fit	Actual	Fit
Air	1					
Tungsten	4.5	4.48	10.1	10.5	0.37	0.38
Copper	6.5	6.47	15.1	14.2	1.42	1.17
Foam	22.5		160		84	

Starting in 1997, we conducted Proton Radiography experiments using the 800-MeV primary beam at LANSCE. Using the accelerator's intense pulsed proton beam, we have been able to take movies (usually 7 pictures, with a current capability of up to 14) of explosively driven, dynamic systems. Because of the low energy of the beam, only relatively thin targets of a few tens of grams per cm^2 can be radiographed. Single pulse radiographs were typically taken using 2×10^9 protons within a 35-ns wide pulse. Dynamic shots of high explosive (HE) during detonation usually had pulses spaced at 1-microsecond intervals.

One of the capabilities that we demonstrated was that we could take radiographs of exploding HE and measure interesting characteristics of the HE. A simple system we studied was a small hemisphere of HE called an onion skin [7]. An onion skin is a hemisphere about 2 inches in diameter with a detonator at the sphere center.

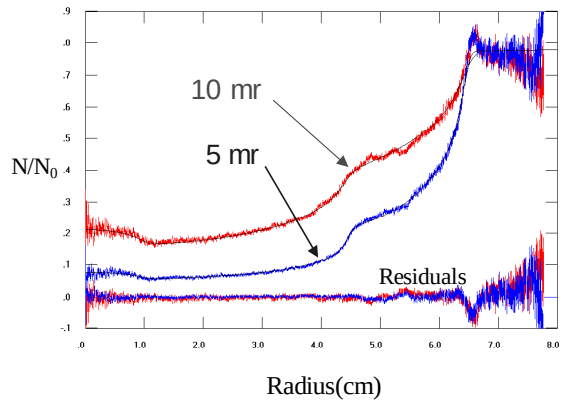

Figure 1, Fits to the transmission data for the FTO. The upper two curves are the measured transmission vs. radius. The bottom curves are the residuals of the two fits.

Figure 2 shows an analysis of an exploding onion skin. The picture is a reconstruction of the density of the material at 1.9 μs time after detonation. This image was obtained using image plates. The burn front in the HE is clearly visible. Comparable multiple images have been obtained with the electronic imaging system.

6 AHF ACCELERATOR

Construction of a proton radiography-based AHF would involve building a new proton accelerator similar in size, energy, and beam intensity to several other proton machines already built [8,9]. Our current studies center on a low-duty-factor 50 GeV synchrotron and 12 isochronous beamlines that converge on a test chamber to provide multiple simultaneous views.

The beam is extracted by a fast kicker and septum magnet. The beam distribution system is based on 4 levels of beam splitting using a combination of electrostatic,

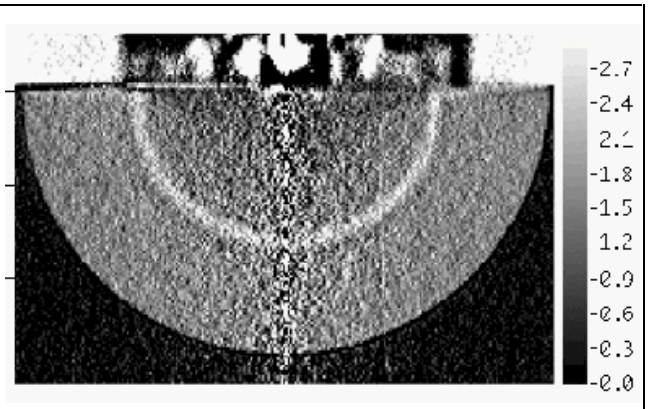

Figure 2. Reconstructed density of an exploding onion skin 1.9 μs time after detonation. The scale on the right is grams per cm^3.

pulsed magnetic, and dc magnet elements. Each beamline is achromatic and isochronous. A single beam bunch extracted from the accelerator will be split 12 ways, and the protons from the bunch will arrive at the target at the same time on each axis. Four of the beam lines will have twice the nominal number of protons, as they will not have the fourth split. These four higher-intensity beam lines would be used for larger field-of-view lenses than the remaining eight.

Each of the beam lines would be outfitted with a lens system as discussed earlier with lens elements both before and after the target chamber. By using large diameter superconducting magnets, such as those in use for the spectrometers at the Thomas Jefferson Lab, it would be possible to have a field of view on each axis up to 50 cm across.

The proton synchrotron typically would have 5 MHz RF accelerating cavities, producing bunches of a few nanoseconds width at 200 ns intervals. With a harmonic number of 20, a motion picture of 20 frames and with a duration equal to the ring period (3-4 microseconds) would be produced if the beam were extracted on a single turn, as with a thyratron-type kicker modulator. A kicker modulator capable of single-pulse extraction in an arbitrary time format, with rise and fall times less than the nearly 200 ns free space between bunches, would make it possible to have nearly arbitrary pulse spacing at the target over times extending up to seconds. This is the mode of operation planned. For a single frame, approximately $1x10^{11}$ protons are required for 1% density measurements. To provide 20 frames, $2x10^{12}$ protons per accelerator cycle are required for each axis, with twice this for the axes that have large lenses. A total of $3.2x10^{13}$ protons per accelerator cycle is required for 12 axes (including four larger-intensity beamlines but excluding losses), a value approximately equal to that which has already been achieved in the Fermilab Main Ring.

A full AHF with up to 12 beam lines would be a costly undertaking. It is thus appropriate to consider staging strategies. A suitable initial step might be to construct a two-axis facility at 50 GeV, which could provide some 3-dimensional information from small-angle stereo views of the object under test. The number of beam lines could be increased later. PRISM-3D (Proton Radiography Intermediate Step Machine with some 3-Dimensional capability) is such a step towards a full future AHF. In this case, $4x10^{12}$ protons per pulse could be obtained by 800 MeV H^- injection from the existing 800 MeV LANSCE linac. In a future upgrade, a booster with an energy of a few GeV could be added to increase the protons per pulse to the level required for full AHF performance. There is a similar proposal from LLNL to build an all-new machine at the Nevada Test Site.

7 SUMMARY

In the three years since the start of serious work on exploring the potential of Proton Radiography, great progress has been made. We have demonstrated Proton Radiography at 800 MeV and 10 GeV. We have shown that we can do material identification. We have operated an 800-MeV dynamic radiographic facility, taking useful data characterizing HE properties. A number of detector projects have been initiated and have produced promising prototypes. The need for more advanced containment systems has been identified and is being addressed. Further experiments are planned to bring us closer to the proposed operating conditions of the AHF.

* LA-UR-99-1542. Work supported by the U.S. Department of Energy under Contracts W-7405-ENG-36 and W-7405-ENG-48 with the University of California, operator of the Los Alamos National Laboratory and Lawrence Livermore National Laboratory and Contract DE-AC02-98CH10886 at Brookhaven National Laboratory operated by Brookhaven Science Associates.

Email: hogan_gary@lanl.gov

8 REFERENCES

[1] H.-J. Ziock, et al., "The Proton Radiography Concept," Proceeding of the Third International Symposium on Development and Application of Semiconductor Tracking Detectors (The Hiroshima Symposium) at Melbourne, December 9-12, 1997, to be published in Nucl. Instrum. Methods, LA-UR-98-1368.

[2] C.T. Mottershead and J. D. Zumbro, “Magnetic Optics for Proton Radiography”, Proceedings of the 1997 Particle Accelerator Conference, Vancouver, B. C., Canada (to be published).

[3] G. J. Yates, et al., "An Intensified/Shuttered Cooled CCD Camera for Dynamic Proton Radiography," Conference on Digital Solid State Cameras: Designs and Applications, SPIE Proceedings Series Vol. 3302, pp. 140-151, January 28-29, 1998, San Jose, California.

[4] R. M. Bionta, H. S. Park et al., "An Energy-Loss Camera Based On Near-Threshold Cerenkov Radiation", Proceedings of American Nuclear Society Annual Meeting, Embedded Topical Meeting on Nuclear Applications of Accelerator Technology Proceedings , 97 (1997).

[5] For more information, contact the author at hogan_gary@lanl.gov.

[6] J. F. Amann, et al., "High-Energy Test of Proton Radiography Concepts (U)," 11th Biennial Nuclear Explosives Design Physics Conference (NEDPC’97), Livermore, California, October 20–24, 1997, Los Alamos National Laboratory document LA-UR-97-4721.

[7] K. B. Morley, et al., "Proof-of-Principle Demonstration of Proton Radiography on a Dynamic Object," 11th Biennial Nuclear Explosives Design Physics Conference (NEDPC’97), Livermore, California, October 20–24, 1997, Los Alamos National Laboratory document LA-CP-98-6.

[8] H. A. Thiessen, "Performance and Facility Issues for Proton Radiography," abstract submitted to the Beams 98 Conference, Haifa, Israel, June 7–12, 1998, Los Alamos National Laboratory document LA-UR-98-561.

[9] F. A. Neri, H. A. Thiessen, and P. L. Walstrom, “Synchrotrons and Beamlines for Proton Radiography”, Proceedings of the 1997 Particle Accelerator Conference, Vancouver, B. C., Canada (to be published).